ORGANOMETALLICS

pubs.acs.org/Organometallics Article

Synthesis and Catalytic Use of Polar Phosphinoferrocene Amidosulfonates Bearing Bulky Substituents at the Ferrocene Backbone

Petr Vosáhlo, Léa Radal, Marine Labonde, Ivana Císařová, Julien Roger, Nadine Pirio, Jean-Cyrille Hierso,* and Petr Štěpnička*

Cite This: *Organometallics* 2021, 40, 1934–1944 Read Online

ACCESS | Metrics & More | Article Recommendations | Supporting Information

ABSTRACT: Anionic phosphinoferrocene amidosulfonates bearing sterically demanding *tert*-butyl substituents in positions 3 and 3′ of the ferrocene scaffold, viz. *rac*-$(Et_3NH)[Fe(\eta^5\text{-}tBuC_5H_3PR_2)(\eta^5\text{-}tBuC_5H_3C(O)NHCH_2SO_3)]$ (R = phenyl, cyclohexyl), were synthesized by amidation of the corresponding phosphinocarboxylic acids, $[Fe(\eta^5\text{-}tBuC_5H_3PR_2)(\eta^5\text{-}tBuC_5H_3CO_2H)]$. These ditopic polar phosphinoferrocenes and their non-*tert*-butylated analogues have been used as ligands to prepare zwitterionic $(\eta^3\text{-allyl})$palladium(II) complexes $[Pd(\eta^3\text{-}C_3H_5)\{Fe(\eta^5\text{-}R'C_5H_3PR_2)(\eta^5\text{-}R'C_5H_3C(O)NHCH_2SO_3)\}]$ (R′ = H, *t*Bu; R = Ph, Cy). Depending on the isolation procedure and crystallization conditions, some complexes were isolated in two isomeric forms which differed in the coordination of the amidosulfonate pendant group, where either amide or sulfonated oxygen ligated the Pd(II) center. The preference for coordination of the amide or sulfonate oxygen atoms has been explained by the interplay of electrostatic and solvation effects and further supported by DFT calculations. The $(\eta^3\text{-allyl})Pd^{II}$ complexes have been applied as defined precatalysts for Pd-catalyzed C−H arylation of an unprotected indole with aryl iodides in polar solvents. Under the optimized reaction conditions at 100 °C in water, C2-arylation proceeded selectively with various aryl iodides to produce the respective 2-arylindoles in acceptable yields at a low catalyst loading (1 mol % Pd) and in the absence of any phase transfer agent. The catalyst possessing *tert*-butyl groups at the ferrocene core and an electron-rich dicyclohexylphosphino group exhibited the best catalytic performance.

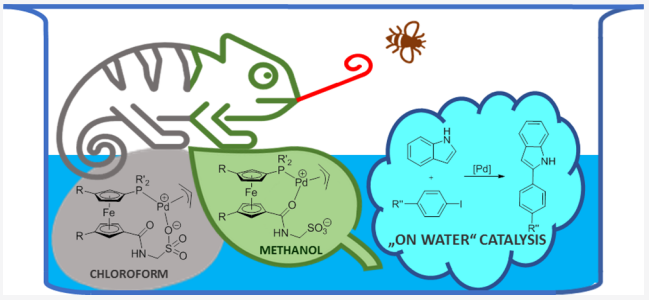

INTRODUCTION

Homogeneous catalysis by transition-metal complexes relies on the development of suitable supporting ligands.[1] Phosphines are particularly attractive due to their tunable steric and electronic properties that can be used to control the course of catalytic processes[2] by means of substituent modification and by incorporation of additional functional groups.[3] The introduction of polar hydrophilic substituents into the ligands is of particular practical importance, as it allows for the transfer of catalytic reactions from purely organic solvents to more innocuous aqueous media.[4] Although numerous polar groups have been used as solubilizing moieties for phosphine ligands (e.g., charged ammonium, guanidinium, and carboxylate fragments), sulfonated phosphines remain the most successful ligands for aqueous catalysis. However, their practical success is partially compromised by the challenging synthesis, as synthetic methods for introducing phosphine and sulfonate moieties are often incompatible due to the sensitivity of the phosphine groups toward oxidation.[4]

To alleviate these problems, we have recently devised an alternative approach based on amide coupling reactions[5] between phosphinocarboxylic acids and aminosulfonic acids, producing the functional amidophosphine ligands $\mathbf{1}^{\mathbf{R}}$ (Scheme 1, left; R = Ph, Cy).[6,7] These coupling reactions proceed with good to excellent yields, employ stable, safe, and readily accessible starting materials, and typically produce pure crystalline products.[8] Utilizing this approach, we synthesized several phosphinoferrocene amidosulfonates, which proved to be useful ligands for catalytic reactions in aqueous systems.[9]

Scheme 1. Phosphinoferrocene Amidosulfonates $\mathbf{1}^{\mathbf{R}}$ and $\mathbf{2}^{\mathbf{R}}$

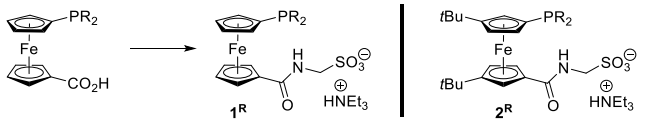

Received: April 21, 2021
Published: June 4, 2021

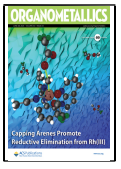

Notably, even a single amidosulfonate tag was sufficient to overcome the hydrophobicity of phosphinoferrocene ligands, which limits their applications in aqueous catalysis.[10]

In this paper, we report the synthesis of new phosphinoferrocene amidosulfonate ligands $\mathbf{2}^{\mathbf{R}}$ containing bulky *tert*-butyl substituents at the ferrocene scaffold (Scheme 1, right; R = Ph, Cy). We have already shown that the introduction of sterically demanding *tert*-butyl substituents to the ferrocene scaffold hinders rotation of the ferrocene cyclopentadienyls, thereby resulting in sterically locked conformations.[11] Such conformations are beneficial for catalysis,[12] partially because of preorganized strong interactions between the donor atoms.[13] The aliphatic substituents also increase electron density at the ferrocene unit and at the attached phosphorus atom and provide steric protection for the phosphine moiety and the ligated, catalytically active metal center. Furthermore, aliphatic substituents render the phosphinoferrocene fragment more hydrophobic and can direct the ligated metal centers toward the organic components of the reaction system, typically the organic reagents. The hydrophilic amidosulfonate tags, meanwhile, can stabilize dispersions formed in water.[4c,14] In this study, the effect of the additional auxiliary substituents was investigated in the challenging Pd-catalyzed C−H arylation of unprotected indoles performed in water, using Pd-allyl complexes stabilized with ligands $\mathbf{1}^{\mathbf{R}}$ and $\mathbf{2}^{\mathbf{R}}$ as the precatalysts.

RESULTS AND DISCUSSION

Synthesis of Polar Phosphinoferrocenes and Their (η^3-Allyl)palladium Complexes. The synthesis of planar-chiral but racemic phosphinoferrocene amidosulfonates $\mathbf{2}^{\mathbf{R}}$, where R = Ph or cyclohexyl (Cy), was performed analogously to the synthesis of compounds $\mathbf{1}^{\mathbf{R}}$ lacking the *tert*-butyl substituents (Scheme 2). The respective starting materials, phosphinocarboxylic acids $\mathbf{5}^{\mathbf{R}}$, were obtained in two steps by sequential lithiation/functionalization of racemic 1,1′-dibromo-3,3′-di-*tert*-butylferrocene (**3**)[15] via phosphine-bromides $\mathbf{4}^{\mathbf{R}}$. Subsequent amidation producing compounds $\mathbf{2}^{\mathbf{Ph}}$ and $\mathbf{2}^{\mathbf{Cy}}$ was achieved by treating acids $\mathbf{5}^{\mathbf{Ph}}$ and $\mathbf{5}^{\mathbf{Cy}}$ successively with 1-hydroxybenztriazole (HOBt), 1-ethyl-3-[3-(dimethylamino)-propyl]carbodiimide (EDC), and aminomethanesulfonic acid in triethylamine/acetonitrile.[9c] This procedure furnished better yields of the coupling products, typically a ca. 95% yield after chromatography, than the method used previously to prepare $\mathbf{1}^{\mathbf{Ph}}$,[6] in which the starting acids were converted to pentafluorophenyl esters that were subsequently reacted with aminomethanesulfonic acid and triethylamine.

Scheme 2. Synthesis of Phosphinoferrocenes $\mathbf{2}^{\mathbf{R}}$ (R = Ph, Cy)[a]

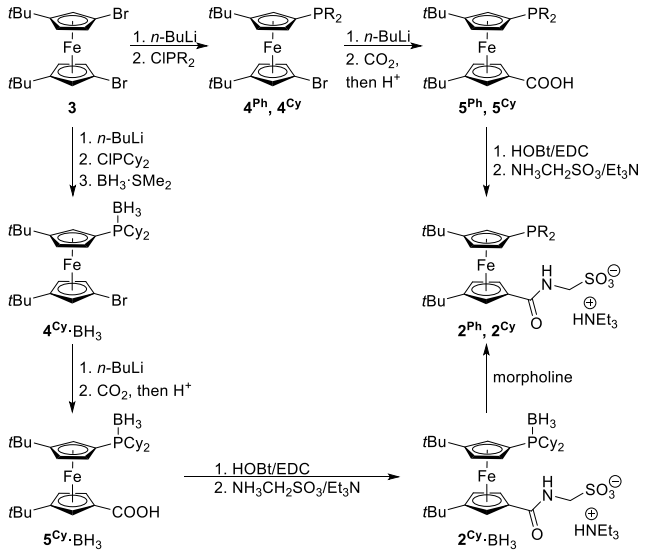

[a]Abbreviations: HOBt, 1-hydroxybenzotriazole; EDC, 1-ethyl-3-[3-dimethylamino)propyl]carbodiimide.

Amide $\mathbf{2}^{\mathbf{Cy}}$ was also synthesized in its P-protected form (Scheme 2), $\mathbf{2}^{\mathbf{Cy}}\cdot BH_3$. In this case, the amidation was performed with the protected acid $\mathbf{5}^{\mathbf{Cy}}\cdot BH_3$, obtained from $\mathbf{4}^{\mathbf{Cy}}\cdot BH_3$.[16] Deprotection was achieved by heating $\mathbf{2}^{\mathbf{Cy}}\cdot BH_3$ in freshly distilled morpholine (65 °C/16 h),[17] providing $\mathbf{2}^{\mathbf{Cy}}$ in 66% yield after chromatography and crystallization. Although this route employs air-stable and easier to handle protected intermediates, it provides a lower overall yield of $\mathbf{2}^{\mathbf{Cy}}$ in comparison to the shorter route, making use of unprotected intermediates (13% vs 38%).

Compounds $\mathbf{2}^{\mathbf{Ph}}$ and $\mathbf{2}^{\mathbf{Cy}}$ were purified by chromatography and crystallization from ethyl acetate, which removed minor amounts of the respective phosphine oxides. The compounds are orange crystalline materials and are stable over extended periods, especially when they are stored under an inert atmosphere. In solution, they undergo slow oxidation under ambient conditions.

The polar ferrocenes $\mathbf{2}^{\mathbf{Ph}}$ and $\mathbf{2}^{\mathbf{Cy}}$ and all reaction intermediates were characterized by NMR and IR spectroscopy, ESI mass spectrometry, and elemental analysis. The solid-state structures of $\mathbf{2}^{\mathbf{Ph}}$ and $\mathbf{2}^{\mathbf{Cy}}\cdot BH_3$ were determined by single-crystal X-ray diffraction analysis (Figure 1 and Table 1; additional structural diagrams are available as Supporting Information).

The molecular structure of $\mathbf{2}^{\mathbf{Ph}}$ (Figure 1) is similar to the structures of $\mathbf{1}^{\mathbf{Ph}}$ and $\mathbf{1}^{\mathbf{Cy}}$ reported previously.[6,9c] It comprises a regular ferrocene moiety, showing similar Fe−C distances and negligible tilting. The functional substituents at positions 1 and 1′ depart by 20° from an eclipsed arrangement. The amide moiety is rotated by 16.5(3)° with respect to its bonding cyclopentadienyl ring so that the nitrogen atom is inclined toward the ferrocene unit. In the crystal, the ions constituting the structure of $\mathbf{2}^{\mathbf{Ph}}$ assemble into closed arrays (Figure 1). Specifically, two amidosulfonate anions forming an enatiomeric pair are linked into dimers located around crystallographic inversion centers by pairs of N1−H1N···O3 hydrogen bonds, and these dimers further serve as H-bond acceptors for two adjacent Et_3NH^+ cations, with the latter acting as bifurcated H-bond donors (N2−H2N···O2/N2−H2N···O4).

Compound $\mathbf{2}^{\mathbf{Cy}}\cdot BH_3$ crystallizes with two structurally independent but essentially identical molecules (see the Supporting Information). Its molecular structure is similar to that of $\mathbf{2}^{\mathbf{Ph}}$. However, the ferrocene units adopt a more opened conformation (i.e., their substituents are more distant; see τ angles in Table 1), and the amide planes depart more from an arrangement coplanar with their parent cyclopentadienyl ring (dihedral angles 34.0(6)/35.5(6)°; in this case, the nitrogen atoms are diverted from the ferrocene unit). The crystal assembly of $\mathbf{2}^{\mathbf{Cy}}\cdot BH_3$ is virtually identical with that of $\mathbf{2}^{\mathbf{Ph}}$.

To examine the catalytic properties of $\mathbf{1}^{\mathbf{R}}$ and $\mathbf{2}^{\mathbf{R}}$, we used these hydrophilic ligands to prepare zwitterionic Pd(allyl) complexes applicable as defined precatalysts (Scheme 3).

Following the procedure used to prepare $\mathbf{6}^{\mathbf{Cy}}$,[9c] we first reacted the ligands with $[Pd(\mu\text{-}Cl)(\eta^3\text{-}C_3H_5)]_2$ to give the

https://doi.org/10.1021/acs.organomet.1c00244
Organometallics 2021, 40, 1934−1944

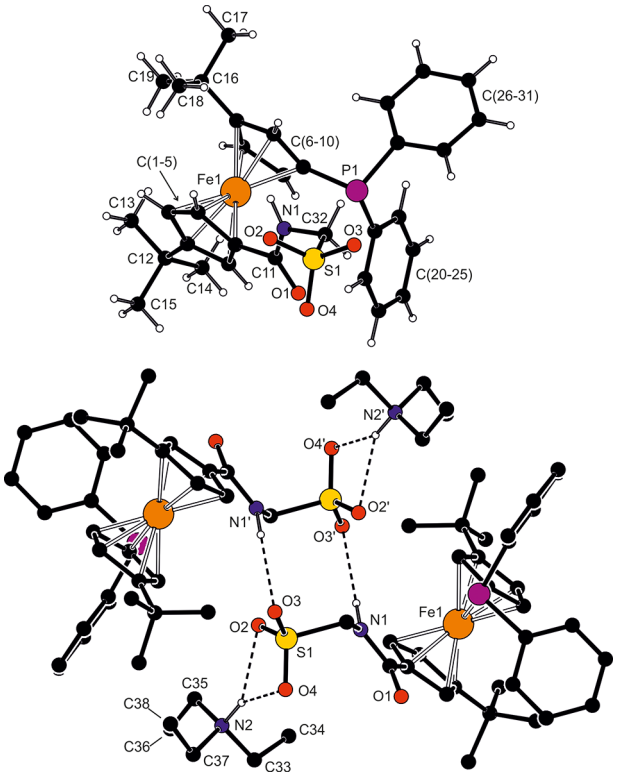

Figure 1. (top) View of the amidosulfonate anion in the structure of 2^{Ph} and (bottom) simplified packing diagram for the same compound. Hydrogen bond parameters: N1···O3 = 3.289(3) Å, N2···O2 = 3.096(3) Å, and N2···O4 = 2.794(3) Å. Note: only one position of the disordered atom C37 is shown for clarity.

Table 1. Selected Distances (Å) and Angles (deg) for 2^{Ph} and 2^{Cy}·BH_3

param[a]	2^{Ph}	2^{Cy}·BH_3 (mol 1/mol 2)[b]
Fe−C (range)	2.045(2)−2.080(2)	2.037(5)−2.081(4)/2.033(5)−2.085(4)
tilt	1.3(1)	4.2(3)/3.9(3)
τ	19.9(2)	54.5(3)/−55.2(3)
C11═O1	1.227(3)	1.226(6)/1.227(6)
C11−N1	1.361(3)	1.360(6)/1.363(6)
N1−C11═O1	122.9(2)	123.6(5)/123.4(5)
S1−O	1.442(2)−1.461(2)	1.453(4)−1.464(3)/1.449(3)−1.464(3)
C32−S1	1.804(2)	1.792(4)/1.797(4)

[a]Definitions: tilt is the dihedral angle between the least-squares cyclopentadienyl planes; τ stands for the torsion angle C1−Cg1−Cg2−C6, where Cg1 and Cg2 denote the centroids of the cyclopentadienyl rings C(1−5) and C(6−10), respectively. [b]Data for two structurally independent molecules. Further parameters: P1−B1= 1.919(6)/1.924(6) Å.

nonisolated phosphine complexes [PdCl(η^3-C_3H_5)(L-κP)] (L = 1^R, 2^R), which were treated with Ag[BF_4] to remove the Pd-bound halide. The resulting zwitterionic complexes were less water soluble than the original phosphinoferrocenes. This was advantageously used during their purification: the partitioning of the crude product between CH_2Cl_2 and water removed $(Et_3NH)[BF_4]$, and the subsequent flash chromatography and crystallization furnished pure complexes 6^R and 7^R as air-stable solids.

Scheme 3. Synthesis of Allylpalladium(II) Complexes 6^R and 7^R

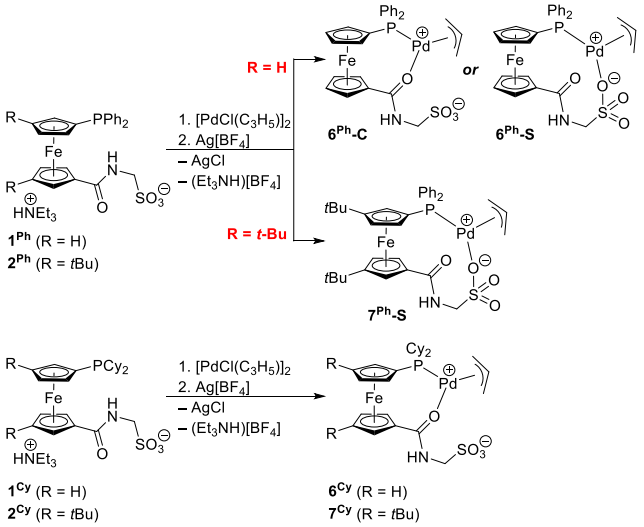

The ligands bearing dicyclohexylphosphine groups produced complexes 6^{Cy} (reported compound[9c]) and 7^{Cy}, wherein the amide oxygen completed the coordination sphere of Pd(II) (N.B.: for 7^{Cy}, the same product resulted upon crystallization from $CHCl_3$/hexane and CH_2Cl_2 + methanol/hexane). Conversely, depending on the crystallization conditions, complex 6^{Ph} was isolated in two coordinative isomeric forms, where either the amide oxygen or the sulfonate oxygen coordinated to palladium (henceforth distinguished as 6^{Ph}-C and 6^{Ph}-S). Whereas 6^{Ph}-C containing a smaller and more rigid P,O-chelate ring was reproducibly obtained from the CH_2Cl_2 + methanol/hexane mixture, the isomeric complex 6^{Ph}-S featuring a charge-supported O→Pd interaction resulted from crystallization with the $CHCl_3$/hexane mixture. Apparently, polar solvents that better solvate the charged sulfonate group favor the formation of 6^{Ph}-C, whereas using a less polar solvent mixture leads to the preferential formation of 6^{Ph}-S. The analogous complex featuring 2^{Ph} was isolated only as a 7^{Ph}-S isomer when either a $CHCl_3$/ethyl acetate mixture or a CH_2Cl_2 + methanol/hexane mixture was used for crystallization. The complexes were structurally authenticated by spectroscopic methods and by an X-ray diffraction analysis (*vide infra*).

The formation of isomers differing in the coordination of the pendant amidosulfonate moiety was analyzed by DFT. In particular, the differences in the Gibbs energy of the C- and S-isomers, $\Delta G = G_S - G_C$, at 298 K (Table 2) suggested that the

Table 2. Gibbs Energy Differences Computed in $CHCl_3$ and Methanol (PCM) between the S- and C-Isomers of 6^{Ph}, 7^{Ph}, and 7^{Cy}

	$\Delta G^{298} = G_S^{298} - G_C^{298}$ (kcal mol^{-1})[a]		
complex	vacuum	$CHCl_3$	methanol
6^{Ph}	−12.83	−4.60	0.028
7^{Ph}	−14.09	−6.19	−1.46
7^{Cy}	2.84	4.05	8.87

[a]Differences in Gibbs free energies at 298 K. A negative ΔG value indicates that the S-isomer is energetically favored over the C-isomer; see the Experimental Section for details. Full computational data are available in the Supporting Information.

https://doi.org/10.1021/acs.organomet.1c00244
Organometallics 2021, 40, 1934−1944

isomer with the sulfonate-bound amidophosphine ligand is favored for 7^{Ph} in both $CHCl_3$ and methanol. Conversely, the C-isomer is preferred for 7^{Cy}, in line with the experimental results. For complex 6^{Ph}, both isomers can be isolated depending on the crystallization conditions. The calculations favored the 6^{Ph}-**S** isomer in $CHCl_3$ as the less polar solvent and revealed a slight preference for the 6^{Ph}-**C** isomer in methanol, again in accordance with the experimental observations. Although the PCM approach[18] used for modeling the solvation effects has limitations for properly accounting for H-bonding interactions, which seem to stabilize the C-isomers via solvation of the uncoordinated sulfonate moiety, our DFT results are consistent with the general experimental trends.

Consistent with the solid-state results, the solution NMR spectra of 6^{R} and 7^{R} displayed markedly broad signals with a significant temperature dependence. This indicated a net fluxionality of the complexes in solution, attributed to ligand shuttling (amide vs sulfonate coordination) and rotation of the Pd-bound allyl moiety. FTIR spectra of the isomeric complexes were quite similar, differing mostly in band intensities. Nonetheless, some diagnostic differences could be observed in the region of carbon stretching modes (see Figure S1).

The structures of 6^{Ph}-**C**·CH_2Cl_2·MeOH and 6^{Ph}-**S**·1.5$CHCl_3$ are displayed in Figure 2; the structures of solvated

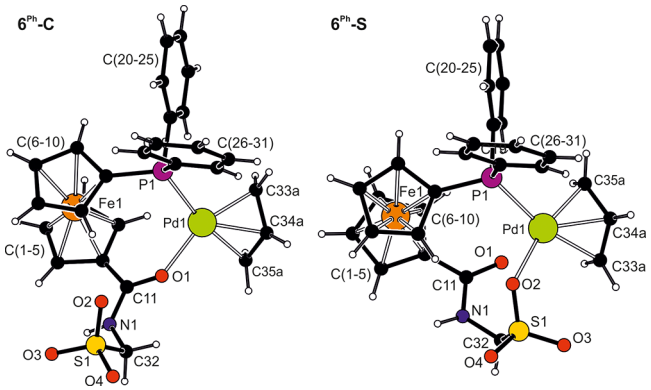

Figure 2. Views of the complex molecules in the structures of 6^{Ph}-**C**·CH_2Cl_2·MeOH and 6^{Ph}-**S**·1.5$CHCl_3$.

7^{Ph} and 7^{Cy} are reported in the Supporting Information, which also provides additional structural diagrams. As stated above, 6^{Ph}-**C**·CH_2Cl_2·MeOH and 6^{Ph}-**S**·1.5$CHCl_3$ differ in coordination of the amidosulfonate moiety. When the molecular structures of 6^{Ph}-**C** and 6^{Ph}-**S** are compared (Table 3), differences in the conformation of the 1,1′-disubstituted ferrocene units can be observed, with the pendant functions approximately 10° closer in 6^{Ph}-**S**. Twisting of the amide moiety in 6^{Ph}-**C** facilitates coordination of the amide oxygen O1, while in 6^{Ph}-**S**, it brings the sulfonate group in the vicinity of the palladium atom (the dihedral angles of the amide plane and ring C(1−5) are 21.6(3)° for 6^{Ph}-**C** and 8.8(2)° in the opposite sense for 6^{Ph}-**S**). In addition, coordination of O2 requires rotation of the sulfonate group along the pivotal C32−S1 bond. Despite these structural changes, the arrangements of the amidosulfonate chain remain similar (cf. the torsion angles C11−N1−C32−S1 of 99.0(3)° in 6^{Ph}-**C** and 95.4(2)° in 6^{Ph}-**S**). The difference in the ligand bite angles, P1−Pd1−O1 vs P1−Pd1−O2, is also small (ca. 5°).

Another notable feature is the positioning of the amide oxygen O1 above the palladium atom in the molecule of 6^{Ph}-**S**

Table 3. Selected Distances (Å) and Angles (deg) for 6^{Ph}-C**·CH_2Cl_2·MeOH and 6^{Ph}-**S**·1.5$CHCl_3$**

param[a]	6^{Ph}-**C** (Y = O1)	6^{Ph}-**S** (Y = O2)
Pd1−P1	2.3086(7)	2.3189(7)
Pd1−Y	2.123(2)	2.165(1)
P1−Pd−Y	101.11(6)	96.16(3)
Fe1−C	2.018(3)−2.075(3)	2.024(2)−2.065(2)
tilt	5.0(2)	4.3(1)
τ	59.3(2)	49.4(1)
C11═O1	1.257(3)	1.232(2)
C11−N1	1.336(4)	1.357(2)
N1−C11═O1	120.4(2)	122.6(2)
S1−O2/3/4	1.443(2)/1.466(2)/ 1.448(3)	1.478(1)/1.451(1)/ 1.449(1)

[a]Parameters are defined as for the free ligand; see footnote to Table 1.

(Pd1···O1 = 2.888(1) Å; the angle between the Pd1···O1 interconnection and the {Pd1,P1,O2} plane is 77.88(5)°), pointing to a possible "axial" interaction.[19] No such contact is detected in the structure of 6^{Ph}-**C**, where the shortest intramolecular distances between Pd1 and sulfonate oxygen atoms exceed 5 Å. The allyl moiety in both structures is disordered over two positions that are approximately mirror images with respect to the {Pd1,O*n*,P1} plane (n = 1, 2).

Catalytic Experiments. Arylindoles are recurring motifs in biologically active molecules and pharmaceuticals.[20] They have been prepared traditionally using cross-coupling strategies.[21] However, the development of direct C−H arylation, while challenging because of the intrinsic strength of this bond, allows direct functionalization of indoles, thus enabling the simple synthesis of aryl-substituted indoles in a more atom-economical process.[22] We used this reaction to assess the properties of palladium catalysts supported by polar ligands 1^{R} and 2^{R} (Scheme 4).

Scheme 4. Direct C−H Arylation of Unprotected Indoles using Allylpalladium Complexes 6^{R} and 7^{R}

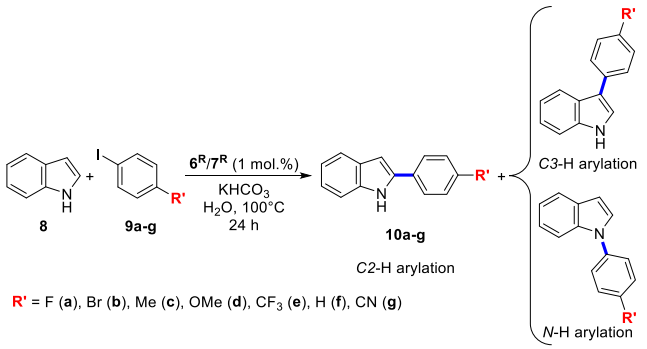

The arylation of unprotected indole **8** was performed in water using complexes 6^{R} and 7^{R} as the defined precatalysts and various *para*-substituted iodoarenes as the arylating agents. Bromoarenes were found to be unreactive during preliminary reaction tests. The initial studies were conducted using 1 mol % of 7^{Ph} for the reaction between **8** and 4-fluoro-1-iodobenzene (**9a**, Scheme 4). As shown in Table 4, the arylation proceeded with a high selectivity, producing nearly exclusively (>99%) C2-arylated product **10a**. We, however, take note of the challenges associated with this coupling reaction under biphasic conditions (see the Experimental Section) since, despite our efforts, the best yields of arylated

https://doi.org/10.1021/acs.organomet.1c00244
Organometallics 2021, 40, 1934−1944

Table 4. Screening of Conditions for the Pd-Catalyzed Indole C2−H Arylation Yielding 2(4-Fluorophenyl)indole (10a)[a]

entry	catalyst	solvent	base	yield of **10a** (%)
1	7^{Ph} (1%)	toluene	$KHCO_3$	<1
2	7^{Ph} (1%)	DMF	$KHCO_3$	<1
3	7^{Ph} (1%)	AcOH	$KHCO_3$	<2
4	7^{Ph} (1%)	ethylene carbonate	$KHCO_3$	<2
5	7^{Ph} (1%)	$MeOC_5H_9$	$KHCO_3$	<2
6	7^{Ph} (1%)	EtOH	$KHCO_3$	<5
7	7^{Ph} (1%)	*tert*-amyl alcohol	$KHCO_3$	<5
8	7^{Ph} (1%)	dioxane	$KHCO_3$	<5
9	7^{Ph} (1%)	dioxane/H_2O[b]	$KHCO_3$	20[c]
10	7^{Ph} (1%)	H_2O	$KHCO_3$	25
11	7^{Ph} (3%)	H_2O	$KHCO_3$	29
12	7^{Ph} (5%)	H_2O	$KHCO_3$	40
13	7^{Ph} (1%)	H_2O	K_2CO_3	15[c]
14	7^{Ph} (1%)	H_2O	KOAc	11

[a]Conditions: 0.5 mmol of **8**, 0.6 mmol of **9a**, 1.5 mmol of base, 2 mL of solvent at 100 °C for 24 h. Yields are from standardized ^{1}H NMR spectra and duplicate experiments. $MeOC_5H_9$ denotes methyl cyclopentyl ether. [b]1:1 (v:v) mixture. [c]Partial loss of selectivity was observed with the formation of ca. 5% of the C3-arylated isomer.

indoles were limited to ca. 50%. As anticipated, the solvent played a crucial role. The use of classical organic solvents such as toluene, DMF, AcOH, and dioxane (Table 4, entries 1−3 and 8) or alcohols (entries 6 and 7) and their more innocuous alternatives (ethylene carbonate and methyl cyclopentyl ether, entries 4 and 5) provided less than 5% conversion. We observed a 20% conversion using a 1:1 mixture of dioxane and water, albeit with a slight loss of selectivity (entry 9). Pleasingly, the use of pure water resulted in a better conversion of 25% and full selectivity (entry 10). Gradually increasing the amount of catalyst 7^{Ph} up to 5 mol % (entries 11 and 12) allowed us to improve this yield to 40% while the C2 selectivity was conserved. Various bases other than $KHCO_3$ were also tested, albeit with detrimental effects on either selectivity or conversion, as illustrated for K_2CO_3 and KOAc (entries 13 and 14).

On the basis of these results, we used water as the solvent and $KHCO_3$ as the base for subsequent experiments aimed at comparing the activity (at 1 mol %) of palladium complexes $\mathbf{6}^R$ and $\mathbf{7}^R$ in the coupling of **8** with functionalized iodoarenes **9b−g** to give arylindoles **10b−g** (Table 5). When the simple allylpalladium(II) complex $[PdCl(\eta^3\text{-}C_3H_5)_2]_2$ in the absence of any ligand (entry 1) or with the "classical" tertiary phosphine ligands PPh_3 and *in situ* deprotected PCy_3 (entries 2 and 3) was used, the arylation of **8** using 4-bromo-1-iodobenzene (**9b**) occurred only marginally. A comparison of the results achieved with palladium complexes stabilized by the polar phosphinoferrocene amidosulfonate ligands with (7^R) or without (6^R) the *t*Bu groups revealed that the activity practically doubled when *t*Bu groups were present (entries 4−7). The presence of dicyclohexylphosphino groups was also beneficial, and complex 7^{Cy} provided **10b** in the best, albeit still modest, yield of 19%. This general trend was confirmed for the reactions producing *p*-tolyl derivative **10c**, since 7^{Cy} provided a 48% yield of this arylindole (entry 11), while 7^{Ph} achieved only a 31% yield (entry 10), and the non-*tert*-butylated counterparts 6^{Cy} and 6^{Ph} were found to be ineffective (entries 8 and 9).

Table 5. Palladium-Catalyzed C2−H Arylation of Indole using Substituted Iodoarenes 9b−g[a]

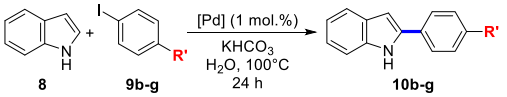

8 9b-g 10b-g

R' = Br (**b**), Me (**c**), OMe (**d**), CF_3 (**e**), H (**f**), CN (**g**)

entry	catalyst	R′	product	yield (%)
1	$[PdCl(C_3H_5)]_2$	Br	**10b**	<2
2	$[PdCl(C_3H_5)]_2/PPh_3$	Br	**10b**	<5
3	$[PdCl(C_3H_5)]_2/PCy_3HBF_4$	Br	**10b**	<5
4	$\mathbf{6}^{Ph}$	Br	**10b**	6
5	$\mathbf{6}^{Cy}$	Br	**10b**	12
6	7^{Ph}	Br	**10b**	14
7	7^{Cy}	Br	**10b**	19
8	$\mathbf{6}^{Ph}$	Me	**10c**	<5
9	$\mathbf{6}^{Cy}$	Me	**10c**	7
10	7^{Ph}	Me	**10c**	31
11	7^{Cy}	Me	**10c**	48
12	7^{Cy}	OMe	**10d**	47
13	7^{Cy}	CF_3	**10e**	40
14	7^{Cy}	H	**10f**	36
15	7^{Cy}	CN	**10g**	15[b]

[a]For conditions, see Table 3. The yields are from standardized ^{1}H NMR spectra and duplicate experiments. [b]A loss of selectivity was observed with the formation of ca. 10% of arylated C3 isomer.

Considering these results, we utilized the most active catalyst 7^{Cy} in reaction tests employing iodoarenes **9d−g** with different substituents. Thus, compounds **10d,e**, incorporating the 4-methoxyphenyl and 4-(trifluoromethyl)phenyl moieties, respectively, were obtained in 47% and 40% yields (entries 12 and 13). The reaction of unsubstituted iodobenzene **9f** proceeded with a lower conversion (36% of **10f**, entry 14), whereas arylation with its electron-poor cyano derivative **9g** (15% of **10g**, entry 15) was more difficult. Surprisingly, catalyst 7^{Cy} showed a higher efficiency for electron-rich iodoarenes, which is rather unusual.[22b] Increasing the reaction time and the amount of catalysts had only marginal effects on the yield of the arylation product.

CONCLUSION

In this paper, we have described the synthesis of two new phosphinoferrocene ligands possessing hydrophilic amidosulfonate pendants and *tert*-butyl substituents that limit the overall molecular mobility. Together with their analogues, which lack the *tert*-butyl substituents, these compounds were used to prepare zwitterionic $(\eta^3\text{-allyl})Pd^{II}$ complexes. The formation of isomers differing in the coordination of the pendant amidosulfonate was noted, controlled by crystallization conditions. This behavior, confirmed by the results of DFT calculations, underlines the hybrid nature of ligands $\mathbf{1}^R$ and $\mathbf{2}^R$, wherein the soft phosphine moiety forms a stronger bond to Pd(II) in comparison to the hard oxygen donors, which in turn results in fluxional coordination. As defined precatalysts, the allylpalladium complexes mediate direct C−H arylation of indole with aryl iodides. Of note is the fairly low catalyst amount (1 mol %), high C2 selectivity, and the absence of the use of an additional phase-transfer agent in this catalytic system.

https://doi.org/10.1021/acs.organomet.1c00244
Organometallics 2021, 40, 1934−1944

EXPERIMENTAL SECTION

Materials and Methods. All reactions were performed under an argon or nitrogen atmosphere by using standard Schlenk techniques. Racemic 1,1′-dibromo-3,3′-di-*tert*-butylferrocene (**3**), $\mathbf{4}^{Ph}$,[15] $\mathbf{4}^{Cy}\cdot BH_3$, $\mathbf{5Cy}\cdot BH_3$, $\mathbf{5}^{Ph}$,[16] $\mathbf{1}^{Ph}$,[6] and $\mathbf{1}^{Cy}$[9c] were prepared as previously reported. Anhydrous THF and dichloromethane were obtained from a Puresolv MD5 solvent purification system. Solvents used for chromatography and crystallizations were of reagent grade and were employed without additional purification. NMR spectra were recorded at 25 °C on Varian UNITY Inova 400 and Bruker Avance 500 and 600 spectrometers. Chemical shifts (δ/ppm) are given relative to internal tetramethylsilane or, alternatively, to residual signals of the deuterated solvents (^{1}H and ^{13}C NMR) and to external 85% aqueous H_3PO_4 (^{31}P NMR). FTIR spectra were recorded on a Nicolet 6700 spectrometer in the range of 400−4000 cm^{-1}. ESI mass spectra were obtained with a Bruker Compact Q-TOF spectrometer. Elemental analyses were performed using a PerkinElmer PE 2400 CHN analyzer or a Thermo Electron Flash EA 1112 Series instrument.

Synthesis of $\mathbf{4}^{Cy}$. Under an argon atmosphere, racemic 1,1′-dibromo-3,3′-di-*tert*-butylferrocene (**3**; 0.912 g, 2.0 mmol) was dissolved in dry THF (10 mL) in an oven-dried, two-necked reaction flask equipped with a stirring bar and an argon inlet. The solution was cooled with an acetone/liquid nitrogen bath to approximately −80 °C before *n*-butyllithium (0.80 mL of 2.5 M in hexanes, 2.0 mmol) was introduced, whereupon the initially yellow solution turned orange-red. The mixture was stirred and cooled for 30 min, and then neat $ClPCy_2$ (0.49 mL, 2.2 mmol) was added dropwise. The resulting mixture was stirred at −80 °C for another 30 min and then gradually warmed to room temperature over 90 min. The crude reaction mixture was concentrated under reduced pressure, and the red oily residue was partitioned between dichloromethane and water (10 mL each). The organic phase was washed with brine, dried over magnesium sulfate, and evaporated, leaving an orange oil, which was taken up with degassed pentane and transferred onto the top of a silica gel column packed in the same solvent. The first yellow band, removed by pentane and containing mostly bromo- and 1,1′-dibromo-3,3′-di-*tert*-butylferrocene (80 mg), was discarded, and the second major orange band eluted by degassed pentane/dichloromethane (4/1) was collected and evaporated, providing pure $\mathbf{4}^{Cy}$ as a yellow-orange foam. Yield: 828 mg (72%).

^{1}H NMR (500 MHz, $CDCl_3$): δ 4.29 (dd, J = 2.4, 1.3 Hz, 1 H, Cp), 4.15−4.13 (m, 1 H, Cp), 4.12 (t, J = 1.5 Hz, 1 H, Cp), 4.03 (dd, J = 2.4, 1.5 Hz, 1 H, Cp), 3.92 (dd, J = 2.5, 1.5 Hz, 1 H, Cp), 3.79 (q, J = 1.4 Hz, 1 H, Cp), 2.00−1.63 (br m, 12 H, Cy), 1.41−0.99 (br m, 10 H, Cy), 1.27 (s, 9 H, *t*Bu), 1.22 (s, 9 H, *t*Bu) ppm. ^{13}C{^{1}H} NMR (126 MHz, $CDCl_3$): δ 105.06 (d, J = 2 Hz, C^{ipso}-*t*Bu of Cp), 101.20 (C^{ipso}-*t*Bu of Cp), 78.83 (d, J = 19 Hz, C^{ipso}-P of Cp), 78.71 (C^{ipso}-Br), 73.10 (d, J = 14 Hz, CH of Cp), 72.73 (d, J = 7 Hz, CH of Cp), 70.06 (CH of Cp), 69.45 (d, J = 2 Hz, CH of Cp), 68.56 (CH of Cp), 64.58 (CH of Cp), 33.86 (d, J = 13 Hz, Cy), 33.38 (d, J = 12 Hz, Cy), 31.83 (d, J = 2 Hz, CH_3 of *t*Bu), 31.78 (CH_3 of *t*Bu), 31.68 (C^{ipso} of *t*Bu), 31.56 (C^{ipso} of *t*Bu), 30.95 (Cy), 30.81 (d, J = 14 Hz, Cy), 30.71 (d, J = 10 Hz, Cy), 30.70 (Cy), 30.48 (d, J = 10 Hz, Cy), 27.57 (d, J = 11 Hz, Cy), 27.50 (d, J = 10 Hz, Cy), 27.47 (Cy), 26.75 (Cy), 26.63 (Cy) ppm. ^{31}P{^{1}H} NMR (202 MHz, $CDCl_3$): δ −8.8 (s) ppm. FTIR (ATR diamond): ν_{max} 2953 m, 2917 vs, 2847 s, 1480 m, 1461 m, 1446 m, 1381 m, 1358 m, 1297 w, 1276 m, 1197 w, 1174 m, 1074 w, 1045 m, 1022 w, 997 w, 917 s, 902, w, 879 s, 843 s, 801 m, 747 w, 675 w, 630 w, 594 w, 550 w, 530 w, 514 s, 497 vs, 478 s, 445 m, 429 m cm^{-1}. Anal. Calcd for $C_{30}H_{46}BrFeP$ (573.4): C, 62.84; H, 8.09. Found: C, 63.09; H, 7.92. ESI-MS: m/z 573 ([M + H]$^+$).

Synthesis of $\mathbf{5}^{Cy}$. Compound $\mathbf{4}^{Cy}$ (0.470 g, 0.82 mmol) was dissolved in dry THF (10 mL) under an argon atmosphere. The solution was cooled in an acetone/liquid nitrogen bath to −80 °C, and *n*-butyllithium (0.56 mL of 1.6 M in hexanes, 0.90 mmol) was added with continuous stirring. The yellow solution turned orange-red after the addition. The resulting mixture was stirred at −80 °C for an additional 30 min before a stream of carbon dioxide was passed through the mixture, first at −80 °C for 2.5 h and then at room temperature for 30 min. Then, the reaction mixture was diluted with dichloromethane (5 mL) and concentrated under reduced pressure. The oily residue was diluted by degassed CH_2Cl_2/MeOH (20/1) and transferred onto the top of a silica gel column packed with the same solvent. The first, minor, yellow band was discarded, and the following, major, red band was collected and evaporated to afford acid $\mathbf{5}^{Cy}$ as a red-orange solid. Yield: 326 mg (74%).

^{1}H NMR (400 MHz, DMSO-d_6): δ 12.07 (br s, 1 H, COOH), 4.59 (br s, 1 H, Cp), 4.35 (br s, 1 H, Cp), 4.21 (br s, 1 H, Cp), 4.09 (br s, 1 H, Cp), 4.05 (br s, 1 H, Cp), 3.88 (br s, 1 H, Cp), 1.95−1.53 (br m, 12 H, Cy), 1.38−0.76 (br m, 10 H, Cy), 1.22 (s, 9 H, *t*Bu), 1.20 (s, 9 H, *t*Bu) ppm. ^{13}C{^{1}H} NMR (101 MHz, DMSO-d_6): δ 172.16 (COOH), 104.67 (C^{ipso}-*t*Bu of Cp), 104.20 (d, J = 3 Hz, C^{ipso}-*t*Bu of Cp), 77.41 (d, J = 21 Hz, C^{ipso}-P of Cp), 71.46 (C^{ipso}-COOH of Cp), 71.01 (br s, CH of Cp), 70.07 (CH of Cp), 69.99 (d, $J \approx$ 14 Hz, CH of Cp), 69.09 (CH of Cp), 68.00 (CH of Cp), 67.70 (CH of Cp), 32.84 (d, J = 13 Hz, Cy), 32.79 (d, J = 13 Hz, Cy), 31.54 (d, J = 3 Hz, CH_3 of *t*Bu), 31.26 (CH_3 of *t*Bu), 31.03 (C^{ipso} of *t*Bu), 30.89 (C^{ipso} of *t*Bu), 30.40 (2 × Cy), 30.27 (d, J = 8 Hz, Cy), 29.96 (d, J = 13 Hz, Cy), 26.79 (Cy), 26.69 (2 × Cy), 26.60 (Cy), 26.19 (Cy), 26.06 (Cy) ppm. ^{31}P{^{1}H} NMR (162 MHz, DMSO-d_6): δ −10.2 (s) ppm. The signal due to the corresponding phosphine oxide appears at δ_P 45.2 (s). FTIR (ATR diamond): ν_{max} 2957 m, 2918 m, 2850 m, 1666 vs (CO), 1489 m, 1479 m, 1464 m, 1446 m, 1390 w, 1366 m, 1339 w, 1313 m, 1263 s, 1173 m, 1070 w, 1039 m, 1022 w, 996 w, 968 m, 939 m, 917 m, 885 w, 852 m, 827 m, 818 m, 783 w, 753 m, 676 w, 630 w, 614 m, 564 m, 532 m, 512 m, 499 s, 479 m, 441 m cm^{-1}. Anal. Calcd for $C_{31}H_{47}FePO_2$ (538.5): C, 69.14; H, 8.80. Found: C, 69.05; H, 8.60. ESI-MS: m/z 539 ([M + H]$^+$).

Synthesis of $\mathbf{2}^{Ph}$. Under argon, acid $\mathbf{5}^{Ph}$ (524.2 mg, 1.0 mmol) and 1-hydroxybenzotriazole (HOBt) (162.1 mg, 1.2 mmol) were suspended in a mixture of dry acetonitrile (19 mL) and triethylamine (1.3 mL). The mixture was cooled in an ice bath and treated with neat *N*-(3-(dimethylamino)propyl)-*N*′-ethylcarbodiimide (EDC; 0.2 mL, 1.2 mmol). After the mixture was stirred at 4 °C for 30 min, solid aminomethanesulfonic acid (888.0 mg, 8.0 mmol) was added, and this mixture was stirred at room temperature for 24 h. Then, it was filtered using a 0.45 μm PTFE syringe filter and evaporated. The obtained crude product was purified by chromatography over a silica gel column using dichloromethane/methanol/triethylamine (90/9/1) as the eluent. The second band was collected and evaporated to give compound $\mathbf{2}^{Ph}$ as an orange solid. Yield: 686.3 mg (95%). Single crystals were obtained from CH_2Cl_2/AcOEt.

^{1}H NMR (400 MHz, CD_2Cl_2): δ 9.86 (br s, 1 H, $HNEt_3$), 7.63−7.55 (m, 2 H, Ph), 7.40−7.35 (m, 3 H, Ph), 7.27−7.16 (m, 5 H, Ph), 6.59 (m, 1 H, NHCO), 4.66 (dd, J = 13.4, 8.1 Hz, 1 H, CH_2), 4.58 (dd, J = 2.6, 1.4 Hz, 1 H, Cp), 4.37 (t, J = 1.5 Hz, 1 H, Cp), 4.20 (dd, J = 2.4, 1.5 Hz, 1 H, Cp), 4.18 (dd, J = 2.6, 1.5 Hz, 1 H, Cp), 4.15 (dt, J = 2.8, 1.5 Hz, 1 H, Cp), 4.14 (dd, J = 13.4, 4.8 Hz, 1 H, CH_2), 3.95 (dt, J = 2.6, 1.3 Hz, 1 H, Cp), 3.07 (dq, J = 7.2, 3.2 Hz, 6 H, CH_3CH_2N), 1.27 (t, J = 1.3 Hz, 9 H, CH_3CH_2N),1.27 (s, 9 H, *t*Bu), 0.99 (s, 9 H, *t*Bu) ppm. ^{13}C{^{1}H} NMR (101 MHz, CD_2Cl_2): δ 170.0 (CONH), 141.0 (d, $^1J_{PC}$ = 12 Hz, C^{ipso} of Ph), 138.1 (d, $^1J_{PC}$ = 10 Hz, C^{ipso} of Ph), 135.5 (d, J = 22 Hz, CH of Ph), 132.7 (d, J = 19 Hz, CH of Ph), 129.7 (CH^{para} of Ph), 128.9 (d, J = 8 Hz, CH of Ph), 128.6 (d, J = 6 Hz, CH of Ph), 128.4 (CH^{para} of Ph), 107.3 (d, J = 6 Hz, C^{ipso}-*t*Bu of Cp), 105.6 (C^{ipso}-*t*Bu of Cp), 76.1 (d, $^1J_{PC}$ = 7 Hz, C^{ipso}-P of Cp), 75.5 (C^{ipso}-CONH of Cp), 73.6 (d, J = 25 Hz, CH of Cp), 71.7 (CH of Cp), 69.7 (CH of Cp), 69.05 (CH of Cp), 68.95 (CH of Cp), 67.2 (d, J = 3 Hz, CH of Cp), 56.1 (CH_2SO_3), 46.5 (CH_3CH_2N), 31.7 (CH of *t*Bu), 31.5 (CH of *t*Bu), 31.2 (C^{ipso} of *t*Bu), 30.7 (C^{ipso} of *t*Bu), 8.8 (CH_3CH_2N) ppm. ^{31}P{^{1}H} NMR (162 MHz, CD_2Cl_2): δ −18.4 (s) ppm. FTIR (Nujol): ν_{max} 3335 w (N−H), 3051 m (N−H), 2720 w, 2688 w, 2525 w, 2360 w, 2342 w, 1717 w, 1656 s (C═O), 1585 w, 1569 w, 1532 m, 1316 w, 1299 w, 1262 m, 1212 m, 1175 m (S═O), 1153 m (P−C), 1104 w, 1087 w, 1079 w, 1071 w, 1036 s (S═O), 971 w (P−C), 930 w, 918 w, 907 w, 895 w, 876 w, 864 w, 849 w, 830 w, 813 w, 766 w, 751 m, 743 m, 699 m, 675 w, 669 w, 626 w, 607 m, 539 m, 530 m, 514 m, 497 m, 479 m, 464 w, 442 m, 424 m, 411 m cm^{-1}. Anal. Calcd for $C_{38}H_{53}N_2PO_4FeS$ (720.28): C, 63.33; H,

https://doi.org/10.1021/acs.organomet.1c00244
Organometallics 2021, 40, 1934−1944

7.41; N, 3.89. Found: C, 63.03; H, 7.15; N, 4.05. ESI-MS: *m*/*z* 618 ([M − $HNEt_3$]$^-$).

Synthesis of 2^{Cy}. An oven-dried, two-necked flask equipped with an argon inlet and stirring bar was charged with the acid 5^{Cy} (619 mg, 1.15 mmol) and HOBt (212 mg, 1.38 mmol), flushed with argon, and sealed. The solids were dissolved by adding dry acetonitrile (20 mL) and degassed triethylamine (8 mL). The solution was cooled on ice, before neat EDC (0.24 mL, 1.38 mmol) was introduced, followed by solid aminomethanesulfonic acid (1.022 g, 9.20 mmol). The reaction mixture was stirred at room temperature for 24 h and then evaporated. The solid residue was taken up with a dichloromethane/methanol/triethylamine (95/4/1) mixture and transferred onto the top of a silica gel column. Elution with the same solvent mixture led to the development of a pale orange band, which was discarded, and a major orange band, which was collected and evaporated. The oily residue was dissolved in hot ethyl acetate (5 mL) and crystallized by cooling to 4 °C. The separated orange crystalline solid was isolated by suction and dried under vacuum. Yield of 2^{Cy}: 596 mg (71%).

^{1}H NMR (400 MHz, DMSO-d_6): δ 9.29 (br s, 1 H, *H*NEt_3), 7.74 (dd, *J* = 7.7, 5.0 Hz, 1 H, NHCO), 4.86 (dd, *J* = 2.6, 1.4 Hz, 1 H, Cp), 4.55 (t, *J* = 1.5 Hz, 1 H, Cp), 4.26 (dd, *J* = 13.0, 7.6 Hz, 1 H, C*H*SO_3), 4.22 (dd, *J* = 2.5, 1.6 Hz, 1 H, Cp), 4.15−4.13 (m, 1 H, Cp), 4.00 (dd, *J* = 2.5, 1.6 Hz, 1 H, Cp), 3.84 (q, *J* = 1.5 Hz, 1 H, Cp), 3.79 (dd, *J* = 13.0, 4.9 Hz, 1 H, C*H*SO_3), 3.08 (q, *J* = 7.3 Hz, 6 H, CH_3CH_2N), 2.10−2.20 (m, 1 H, Cy), 1.95−0.85 (m, 20 H, Cy), 1.21 (s, 9 H, *t*Bu), 1.18 (t, *J* = 7.3 Hz, 9 H, CH_3CH_2N), 1.17 (s, 9 H, *t*Bu), 0.68−0.55 (m, 1 H, Cy) ppm. ^{13}C{^{1}H} NMR (101 MHz, DMSO-d_6): δ 168.45 (CONH), 104.46 (d, *J* = 4 Hz, C^{ipso}-*t*Bu of Cp), 103.76 (C^{ipso}-*t*Bu of Cp), 76.11 (d, *J* = 20 Hz, C^{ipso}-P of Cp), 75.59 (C^{ipso}-CONH of Cp), 70.39 (d, *J* = 20 Hz, CH of Cp), 69.46 (CH of Cp), 69.30 (CH of Cp), 68.72 (CH of Cp), 67.50 (CH of Cp), 66.29 (CH of Cp), 55.50 (CH_2SO_3), 45.65 (CH_3CH_2N), 33.28 (d, *J* = 15 Hz, Cy), 32.38 (d, *J* = 12 Hz, Cy), 31.79 (d, *J* = 3 Hz, CH_3 of *t*Bu), 31.55 (C^{ipso} of *t*Bu), 31.50 (CH_3 of *t*Bu), 31.37 (C^{ipso} of *t*Bu), 30.73 (d, *J* = 17 Hz, Cy), 30.38 (Cy), 30.29 (Cy), 29.38 (d, *J* = 10.5 Hz, Cy), 28.69 (br s, Cy), 27.01 (d, *J* = 4 Hz, Cy), 26.89 (d, *J* = 5 Hz, Cy), 26.69 (d, *J* = 8 Hz, Cy), 26.62 (d, *J* = 6 Hz, Cy), 26.21 (Cy), 26.10 (Cy), 8.57 (CH_3CH_2N) ppm. ^{31}P{^{1}H} NMR (162 MHz, DMSO-d_6): δ −10.0 (s) ppm. The signal of the respective phosphine oxide is observed at δ_P 45.2 (s). FTIR (ATR diamond): ν_{max} 3345 w, 3082 w, 2915 m, 2848 m, 2696 w, 1651 m (CO), 1522 m, 1484 m, 1449 m, 390 w, 1363 w, 1313 w, 1256 m, 1233 m, 1209 m, 1163 s, 1075 w, 1035 s, 969 w, 930 w, 919 w, 897 w, 848 m, 814 w, 791 w, 772 w, 750 w, 669 w, 598 m, 532 m, 519 m, 487 m, 441 w cm^{-1}. Anal. Calcd for $C_{38}H_{65}N_2FeO_4PS$ (732.8): C, 62.28; H, 8.94; N, 3.82. Found: C, 61.90; H, 8.68; N, 3.65. ESI-MS: *m*/*z* 630 ([M − $HNEt_3$]$^-$).

Synthesis of 2^{Cy}·BH_3. Compound 2^{Cy}·BH_3 was prepared similarly, starting from 5^{Cy}·BH_3 (1.10 g, 2.0 mmol) and HOBt (0.324 g, 2.4 mmol) in dry acetonitrile (38 mL) and triethylamine (2.6 mL). The suspension was cooled in an ice bath and treated with neat EDC (0.40 mL, 2.4 mmol). The mixture was stirred at 0 °C for 30 min, and aminomethanesulfonic acid (1.78 g, 16.0 mmol) was added. The resultant mixture was stirred at room temperature for 24 h and filtered through a 0.45 μm PTFE syringe filter, and the filtrate was evaporated. The crude product was purified by chromatography over silica gel and eluted with a dichloromethane/methanol/triethylamine mixture (90/9/1). The main second band was collected and evaporated, leaving 2^{Cy}·BH_3 as an orange solid. Yield: 1.42 g (95%). Single crystals were obtained from CH_2Cl_2/AcOEt.

^{1}H NMR (400 MHz, CD_2Cl_2): δ 6.62−6.58 (m, 1 H, NH), 4.75 (dd, *J* = 2.6, 1.4 Hz, 1 H, Cp), 4.67 (t, *J* = 1.5 Hz, 1 H, Cp), 4.58 (dd, *J* = 13.5, 7.5 Hz, 1 H, CH_2), 4.40−4.37 (m, 1 H, Cp), 4.35 (dd, *J* = 2.6, 1.6 Hz, 1 H, Cp), 4.31−4.29 (m, 1 H, Cp), 4.23 (dd, *J* = 13.5, 5.5 Hz, 1 H, CH_2), 4.10 (q, *J* = 1.5 Hz, 1 H, Cp), 3.90−3.35 (very br s, 1H, NH of $HNEt_3$), 3.01 (q, *J* = 7.3 Hz, 6 H, CH_3CH_2N), 1.99−1.61 (m, 12 H, Cy), 1.45−0.98 (m, 12 H, Cy), 1.29 (s, 9 H, *t*Bu), 1.26 (s, 9 H, *t*Bu), 1.25 (t, *J* = 7.3 Hz, 9 H, CH_3CH_2N), 0.85−0.12 (m, 3 H, BH_3) ppm. ^{13}C{^{1}H} NMR (101 MHz, CD_2Cl_2): δ 169.88 (CONH), 106.84 (d, *J* = 6 Hz, C^{ipso}-*t*Bu of Cp), 106.61 (C^{ipso}-*t*Bu of Cp), 76.05 (C^{ipso}-CONH of Cp), 72.44 (d, *J* = 5 Hz, CH of Cp), 70.96 (d, *J* = 7 Hz, CH of Cp), 70.50 (d, $^1J_{PC}$ = 55 Hz, C^{ipso}-P of Cp), 69.93 (CH of Cp), 69.48 (CH of Cp), 69.06 (CH of Cp), 66.81 (CH of Cp), 56.17 (CH_2SO_3), 46.51 (CH_3CH_2N), 33.51 (d, *J* = 10 Hz, Cy), 33.18 (d, *J* = 10 Hz, Cy), 32.20 (CH of *t*Bu), 31.75 (CH of *t*Bu), 31.17 (C^{ipso} of *t*Bu), 31.03 (C^{ipso} of *t*Bu), 28.19 (Cy), 28.14 (Cy), 27.95 (Cy), 27.84 (Cy), 27.40 (d, *J* = 11 Hz, Cy), 27.39 (Cy), 27.27 (Cy), 27.21 (d, *J* ≈ 12 Hz, Cy), 26.52 (Cy), 26.47 (Cy), 9.27 (CH_3CH_2N) ppm. ^{31}P{^{1}H} NMR (162 MHz, CD_2Cl_2): δ 25.2 (br s) ppm. FTIR (Nujol): ν_{max} 3412 m, 2377 m (borane), 2274 w, 1648 m (CO), 1540 m, 1263 m, 1202 m, 1178 m, 1062 m, 1038 m, 972 w, 931 w, 920 w, 903 w, 890 w, 853 w, 822 w, 755 w, 722 w, 670 w, 616 w, 596 w, 519 w, 473 w, 435 w cm^{-1}. Anal. Calcd for $C_{38}H_{68}N_2BFePO_4S$ (746.7): C, 61.13; H, 9.18; N, 3.75. Found: C, 61.07; H, 9.35; N, 3.35. ESI-MS: *m*/*z* 644 ([M − $HNEt_3$]$^+$).

Deprotection of 2^{Cy}·BH_3. Compound 2^{Cy}·BH_3 (691 mg, 1.0 mmol) was dissolved in morpholine (7 mL). The mixture was degassed by three freeze−pump−thaw cycles and then heated at 65 °C for 16 h before evaporation under reduced pressure. The oily residue was transferred onto the top of a silica gel column packed in degassed CH_2Cl_2/MeOH/Et_3N (100/5/5). A single orange band was eluted with degassed CH_2Cl_2/MeOH (20/1) and evaporated. The gummy residue was crystallized from hot ethyl acetate (ca. 5 mL) to produce 2^{Cy} as an orange-red microcrystalline solid (487 mg, 66%).

Synthesis of 6^{Ph}. Solid [Pd(μ-Cl)(η^3-C_3H_5)]$_2$ (18.3 mg, 0.05 mmol) and 1^{Ph} (60.9 mg, 0.10 mmol) were dissolved in dry dichloromethane (5 mL). After the mixture was stirred for 30 min, a solution of silver(I) tetrafluoroborate (19.4 mg, 0.10 mmol) in MeOH (1 mL) was added, causing immediate separation of an off-white precipitate (AgCl) and a color change from orange to orange-brown. The resulting mixture was stirred for 1 h and filtered through a plug of Dicalite filter aid. The filtrate was evaporated and the residue redissolved in dichloromethane (5 mL). The solution was washed three times with distilled water (5 mL each) to remove $Et_3NH[BF_4]$, dried over magnesium sulfate, and evaporated. The residue was taken up with dichloromethane/methanol (20/1) and filtered through a pad of silica gel to provide pure 6^{Ph} as an orange solid after evaporation. Crystallization by liquid-phase diffusion of pentane into a solution of the complex in CH_2Cl_2/MeOH (20/1) gave orange crystals. Yield: 54 mg (82%). Crystals used for X-ray diffraction analysis were grown from chloroform/pentane.

^{1}H NMR (400 MHz, $CDCl_3$, 25 °C): δ 7.49−7.36 (m, 10 H, Ph), 7.32 (t, *J* = 6.7 Hz, 1 H, NH), 5.78 (qi, *J* = 9.9 Hz, 1 H, C_3H_5), 5.60−5.00 (very br s, 1 H, C_3H_5), 5.00−4.30 (br s, 2 H of Cp and 1 H of C_3H_5), 4.84 (t, *J* = 1.9 Hz, 2 H, Cp), 4.49 (br s, 2 H, Cp), 4.21 (t, *J* = 1.9 Hz, 2 H, Cp), 3.60−2.60 (very br s, 2 H, C_3H_5 or CH_2) ppm. ^{1}H NMR (400 MHz, $CDCl_3$, 50 °C): δ 7.51−7.36 (m, 10 H, Ph), 7.06 (t, *J* = 6.7 Hz, 1 H, NH), 5.76 (qi, *J* = 9.9 Hz, 1 H, C_3H_5), 4.75 (t, *J* = 1.9 Hz, 2 H, Cp), 4.68 (br s, 2 H, C_3H_5 or Cp), 4.66 (br s, 2 H, C_3H_5 or Cp), 4.51 (br t, *J* = 1.8 Hz, 2 H, Cp), 4.35−3.09 (br s, 2 H, C_3H_5 or CH_2), 4.19 (t, *J* = 1.9 Hz, 2 H, Cp) ppm. At both temperatures, signals due to two hydrogen atoms of C_3H_5 and/or CH_2SO_3 were not observed due to extensive broadening. ^{31}P{^{1}H} NMR (161 MHz, $CDCl_3$, 25 °C): δ 14.8 (s) ppm. FTIR of 6^{Ph}-**C** (DRIFTS, KBr): ν_{max} 3312 w, 3233 w, 3088 w, 1641 m, 1596 m, 1541 m, 1480 w, 1436 m, 1402 w, 1387 w, 1314 w, 1257 m, 1228 m, 1220 m, 1185 m, 1154 s, 1099 w, 1074 w, 1044 m, 1035 w, 963 w, 912 w, 897 w, 844 w, 828 w, 751 m, 694 m, 611 m, 541 w, 532 m, 516 s, 490 m, 469 m, 450 m cm^{-1}. FTIR of 6^{Ph}-**S** (DRIFTS, KBr): ν_{max} 3319 s, 3116 w, 300 w, 3085 w, 3057 m, 2955 m, 2871 w, 1641 s, 1586 w, 1538 m, 1532 m, 1481 w, 1456 w, 1435 m, 1402 w, 1388 w, 1379 w, 1363 w, 1312 m, 1258 s, 1214 m, 1155 vs, 1099 m, 1074 w, 1058 w, 1027 m, 1019 m, 911 w, 892 w, 869 w, 857 w, 823 w, 817 w, 747 m, 705 m, 694 m, 668 w, 626 w, 613 m, 590 w, 583 w, 552 w, 541 w, 528 m, 514 m, 494 m, 480 w, 469 m, 451 w, 439 m, 430 w cm^{-1}. Anal. Calcd for $C_{27}H_{26}NFeO_4PPdS{\cdot}0.3CH_2Cl_2$ (679.28): C, 48.27; H, 3.95; N, 2.06. Found: C, 48.34; H, 4.03; N, 2.12. The amount of clathrated solvent was verified by NMR analysis (δ_H 5.30). HR ESI-MS calc. for $C_{27}H_{26}NNaPO_4FeSPd$ ([M + Na]$^+$): 675.9597, found: 675.9613.

https://doi.org/10.1021/acs.organomet.1c00244
Organometallics 2021, 40, 1934−1944

Synthesis of 6^{Cy}. Compound 6^{Cy} was prepared similarly, using $[Pd(\mu\text{-}Cl)(\eta^3\text{-}C_3H_5)]_2$ (17.5 mg, 0.048 mmol) and 1^{Cy} (59.5 mg, 0.096 mmol) in dry dichloromethane (5 mL) and $Ag[BF_4]$ (18.7 mg, 0.096 mmol) in MeOH (1 mL). Purification and crystallization as described above produced 6^{Cy} as an orange crystalline solid. Yield: 51 mg (80%).

^{1}H NMR (400 MHz, $CDCl_3$, 25 °C): δ 7.87 (t, J = 6.7 Hz, 1 H, NH), 5.71 (qi, J = 9.9 Hz, 1 H, C_3H_5), 4.96 (br m, 2 H, Cp), 4.74 (br m, 2 H, Cp), 4.62 (br d, J = 6.6 Hz, 2 H, CH_2), 4.53 (br m, 2 H, Cp), 4.41 (br m, 2 H, Cp). 4.00−3.20 (very br s, 2 H, C_3H_5), 3.20−2.50 (very br s, 2 H, C_3H_5), 2.09−1.65 (m, 11 H, Cy), 1.41−1.09 (m, 11 H, Cy) ppm. $^{31}P\{^1H\}$ NMR (161 MHz, $CDCl_3$, 25 °C): δ 27.3 (s) ppm. The data agree with those found in the literature.[9c]

Synthesis of 7^{Ph}. The solids $[Pd(\mu\text{-}Cl)(\eta^3\text{-}C_3H_5)]_2$ (56.0 mg, 0.15 mmol) and 2^{Ph} (216.2 mg, 0.30 mmol) were dissolved in dry dichloromethane (10 mL). After the mixture was stirred for 30 min, a solution of $Ag[BF_4]$ (59.6 mg, 0.30 mmol) in MeOH (1.5 mL) was added, resulting in the separation of an off-white solid (AgCl) and a color change from orange to orange-brown. The resulting mixture was stirred for 1 h and filtered through a cotton plug. The filtrate was evaporated and redissolved in dichloromethane (10 mL). The solution was washed three times with 10 mL of distilled water to remove $Et_3NH[BF_4]$, dried over magnesium sulfate, and evaporated. The residue was dissolved in dichloromethane/methanol (20/1) and filtered through a pad of silica gel. The filtrate was evaporated, and the residue was crystallized by dissolving in dichloromethane/methanol (20/1, 5 mL) and layering with pentane (ca. 15 mL). The crystals, which separated for several days, were filtered off and dried under vacuum to give 7^{Ph} as an orange crystalline solid. Yield: 196 mg (85%).

^{1}H NMR (400 MHz, $CDCl_3$, 25 °C): δ 7.84−7.75 (m, 2 H, Ph), 7.53−7.47 (m, 3 H, Ph), 7.37−7.24 (m, 3 H, Ph), 7.06−6.98 (m, 2 H, Ph), 6.62 (dd, J = 10.8, 2.2 Hz, 1 H, NH), 5.79 (br s, 1 H, C_3H_5), 5.63 (br s, 1 H, Cp), 5.30 (dd, J = 13.6, 11.0 Hz, 1 H, C_3H_5), 4.77 (br s, 1 H, Cp), 4.71 (dd, J = 2.7, 1.4 Hz, 1 H, Cp), 4.27 (dd, J = 2.6, 1.8 Hz, 1 H, Cp), 4.17 (dd, J = 2.5, 1.6 Hz, 1 H, Cp), 4.10−2.50 (very br s, 1 H, C_3H_5 or CH_2SO_3), 3.97 (dd, J = 13.7, 2.6 Hz, 1 H, C_3H_5), 3.72 (td, J = 2.1, 1.4 Hz, 1 H, Cp), 1.37 (s, 9 H, *t*Bu), 0.82 (s, 9 H, *t*Bu) ppm. ^{1}H NMR (400 MHz, $CDCl_3$, 50 °C): δ 7.84−7.77 (m, 2 H, Ph), 7.51−7.47 (m, 3 H, Ph), 7.36−7.24 (m, 3 H, Ph), 7.06−6.99 (m, 2 H, Ph), 6.54 (dd, J = 11.1, 2.1 Hz, 1 H, NH), 5.78 (qi, J = 9.8 Hz, 1 H, C_3H_5), 5.64 (dt, J = 3.0, 1.5 Hz, 1 H, Cp), 5.27 (dd, J = 13.6, 10.9 Hz, 1 H, C_3H_5), 4.75 (br s, 1 H, Cp), 4.70 (dd, J = 2.8, 1.4 Hz, 1 H, Cp), 4.25 (dd, J = 2.7, 1.7 Hz, 1 H, Cp), 4.16 (dd, J = 2.5, 1.6 Hz, 1 H, Cp), 3.95 (dd, J = 13.6, 2.6 Hz, 1 H, C_3H_5), 3.73 (td, J = 2.2, 1.4 Hz, 1 H, Cp), 4.40−3.22 (very br s, 1 H, C_3H_5 or CH_2SO_3), 1.37 (s, 9 H, *t*Bu), 0.83 (s, 9 H, *t*Bu) ppm. At both temperatures, the signals of three hydrogen atoms from C_3H_5 and CH_2SO_3 could not be unequivocally identified due to extensive broadening. $^{31}P\{^1H\}$ NMR (161 MHz, $CDCl_3$, 25 °C): δ 14.2 (s) ppm. FTIR (DRIFTS, KBr): ν_{max} 3504 w, 3441 w, 3339 w, 3097 w, 3058 w, 2963 m, 2905 w, 2867 w, 1643 m, 1526 m, 1482 m, 1459 w, 1435 m, 1400 w, 1365 m, 1314 w, 1270 m, 1258 s, 1214 w, 1179 m, 1150 vs, 1097 w, 1080 w, 1013 m, 973 w, 920 w, 856 w, 824 w, 750 m, 728 w, 704 w, 697 s, 616 w, 588 w, 560 w, 539 m, 524 m, 509 s, 493 m, 481 m, 440 w cm^{-1}. Anal. Calcd for $C_{35}H_{42}NFeO_4PPdS\cdot0.8CH_2Cl_2$ (833.96): C, 51.56; H, 5.27; N, 1.68. Found: C, 51.42; H, 5.43; N, 1.72. The amount of residual solvent was confirmed by NMR analysis (δ_H 5.30). HR ESI-MS: calcd for $C_{35}H_{42}FeNNaO_4PPdS$ ($[M + Na]^+$) 788.08486, found 788.08674.

Synthesis of 7^{Cy}. Compound 7^{Cy} was prepared in an analogous manner starting from 2^{Cy} (219.9 mg, 0.30 mmol). Crystallization by dissolving the crude product in dichloromethane/methanol (20/1, 3 mL) and layering with pentane (10 mL) provided 7^{Cy} as an orange-red crystalline solid. Yield: 194 mg (83%).

^{1}H NMR (400 MHz, $CDCl_3$, 25 °C): δ 6.99 (br s, 1 H, NH), 5.70 (qi, J = 9.5 Hz, 1 H, C_3H_5), 5.26 (dt, J = 2.8, 1.5 Hz, 1 H, Cp), 5.13 (dd, J = 13.6, 10.5 Hz, 1 H, C_3H_5), 4.80 (br s, 1 H, Cp), 4.73 (br s, 1 H, Cp), 4.32 (dd, J = 2.7, 1.8 Hz, 1 H, Cp), 4.24 (br s, 1 H, Cp), 4.14 (dd, J = 2.4, 1.6 Hz, 1 H, Cp), 3.97 (dd, J = 13.6, 2.0 Hz, 1 H, C_3H_5), 3.49 (br s, 2 H, CH_2SO_3), 2.68−2.58 (m, 1 H, Cy), 1.33 (s, 9 H, *t*Bu), 1.23 (s, 9 H, *t*Bu), 2.20−0.64 (m, 21 H, Cy) ppm. Two signals with integral intensities corresponding to two hydrogen atoms at C_3H_5 were not observed due to broadening. ^{1}H NMR (400 MHz, $CDCl_3$, 50 °C): δ 6.74 (br d, J = 10.7 Hz, 1 H, NH), 5.67 (qi, J = 9.9 Hz, 1 H, C_3H_5), 5.28 (dt, J = 2.8, 1.5 Hz, 1 H, Cp), 5.12 (dd, J = 13.6, 10.6 Hz, 1 H, C_3H_5), 4.80−4.04 (very br s, 1 H, C_3H_5), 4.75 (dd, J = 2.7, 1.4 Hz, 1 H, Cp), 4.72 (t, J = 1.6 Hz, 1 H, Cp), 4.30 (dd, J = 2.7, 1.8 Hz, 1 H, Cp), 4.23 (dt, J = 2.5, 1.2 Hz, 1 H, Cp), 4.14 (dd, J = 2.5, 1.6 Hz, 1 H, Cp), 4.04−3.31 (very br s, 1 H, C_3H_5) 3.94 (dd, J = 13.5, 2.9 Hz, 1 H, C_3H_5), 3.48 (br s, 2 H, CH_2SO_3), 2.66−2.57 (m, 1 H, Cy), 2.24−0.70 (m, 21 H, Cy), 1.34 (s, 9 H, *t*Bu), 1.24 (s, 9 H, *t*Bu) ppm. $^{31}P\{^1H\}$ NMR (161 MHz, $CDCl_3$, 25 °C): δ 27.2 (br s) ppm. FTIR (DRIFTS, KBr): ν_{max} 3599 w, 3450 w, 3240 m, 3102 w, 3062 w, 2958 m, 2930 s, 2853 m, 1644 w, 1574 s, 1484 w, 1456 m, 1448 m, 1407 w, 1389 w, 1365 m, 1332 m, 1290 w, 1271 m, 1223 m, 1197 m, 1178 s, 1155 m, 1114 w, 1092 w, 1038 m, 1007 w, 966 w, 918 w, 907 w, 890 w, 855 w, 831 w, 813 w, 771 w, 746 m, 679 w, 616 m, 592 w, 539 w, 525 m, 508 m, 493 m, 478 w cm^{-1}. Anal. Calcd for $C_{35}H_{54}NFeO_4PPdS\cdot0.3CH_2Cl_2$ (803.6): C, 52.76; H, 6.85; N, 1.74. Found: C, 52.85; H, 6.84; N, 1.56. The amount of residual solvent was confirmed by NMR analysis (δ_H 5.30). HR ESI-MS: calcd for $C_{27}H_{26}NNaPO_4FeSPd$ ($[M + Na]^+$) 800.17876, found 800.18026.

Catalytic Experiments. In air, the preformed catalyst 7^R or 6^R (1 mol % based on indole) was placed into a Schlenk tube equipped with a stirring bar, followed by indole (58.6 mg, 0.50 mmol) and $KHCO_3$ as the base (150 mg, 1.50 mmol; 3 equiv). Solid iodoarenes (0.60 mmol, 1.2 equiv) were added at this stage before deoxygenating the solid mixture through three vacuum/argon cycles. Liquid iodoarenes were added by syringe after deoxygenation. Next, 2 mL of degassed water (bubbled for 30 min with argon) was added and the Schlenk tube was transferred into a preheated oil bath (100 ± 2 °C) and stirred for 24 h. All reactions were clearly biphasic, potentially limiting the mass transfer, which was also the limitation for the conversion. The reaction was terminated by cooling to room temperature and adding dichloromethane (5 mL). The organic phase was separated, and the water phase was washed two times using 5 mL of dichloromethane. The combined organic phases were dried over $MgSO_4$ and evaporated after filtration. The resulting crude products were dissolved in DMSO-d_6 and analyzed by NMR spectroscopy.

X-ray Crystallography. Full-sphere diffraction data ($\pm h,\pm k,\pm l$, θ_{max} = 27.5°) were collected with a Bruker D8 VENTURE Kappa Duo diffractometer equipped with a Cryostream Cooler (Oxford Cryosystems) using Cu Kα (λ = 1.54178 Å; only for $2^{Cy}\cdot BH_3$) or Mo Kα (λ = 0.71073 Å; all other compounds) radiation. The structures were obtained using direct methods (SHELXT, recent version[23]) and subsequently refined by full-matrix least squares based on F^2 (SHELXL-2017[24]). Non-hydrogen atoms were refined with anisotropic displacement parameters. Amide NH (except for 6^{Ph}-C·CH_2Cl_2·MeOH) and BH_3 hydrogens were identified on the difference electron density maps and refined as riding atoms with U_{iso}(H) set to 1.2U_{eq} of their bonding atom. Hydrogen atoms in the CH_n groups were placed in their theoretical positions and refined similarly. Particular details are as follows.

Compound $2^{Cy}\cdot BH_3$ crystallized as a three-component, non-merohedral twin. The refined contributions of the three domains were approximately 0.661:0.214:0.125. In the structure of 2^{Ph}, one ethyl substituent of the Et_3NH^+ cation had to be refined over two positions due to disorder. Similarly, the allyl moieties in all $Pd(\eta^3$-allyl) complexes reported here were disordered and had to be modeled over two positions, rotated approximately 180° along the Pd−allyl axis. The solvent molecules in the structure of $7^{Cy}\cdot 0.125CH_2Cl_2\cdot 0.875$ MeOH occupy the same space and were refined so that their occupancies summed up to 1. Finally, the solvent molecules in the structures of 6^{Ph}-C·CH_2Cl_2·MeOH and 6^{Ph}-S·$1.5CHCl_3$ were disordered within structural voids and could not be satisfactorily incorporated in the structure model. Therefore, their contribution to the overall scattering was eliminated using PLATON SQUEEZE.[25] The removed electron density was in good agreement with the expected value (106 electrons for 6^{Ph}-C·CH_2Cl_2·MeOH with

https://doi.org/10.1021/acs.organomet.1c00244
Organometallics 2021, 40, 1934−1944

120 expected, and 696 electrons for 6^{Ph}-S·1.5$CHCl_3$ with 696 electrons expected).

Selected crystallographic data and refinement parameters are available in Table S1 in the Supporting Information. All geometric data and structural diagrams were obtained using a recent version of the PLATON program.[26] The numerical values were rounded to one decimal place with respect to their estimated standard deviations (ESDs). Parameters pertaining to atoms in geometrically constrained positions (hydrogens) are given without ESDs.

DFT Calculations. Density functional theory calculations were performed using Gaussian 16, revision C.01.[27] The reported energies correspond to Gibbs free energies obtained after full geometry optimizations, starting from atomic coordinates determined by X-ray diffraction analysis where possible (the more populated orientation of the π-coordinated allyl group was used), using the PBE0 density functional[28] combined with the Stuttgart–Dresden core potential[29] for Fe and Pd and the Jul-cc-pVDZ[30] basis set for the remaining atoms. The solvent effects were approximated using the polarized continuum model (PCM).[18] Cartesian coordinates of the DFT-optimized structures are available in the Supporting Information.

■ ASSOCIATED CONTENT

Supporting Information

The Supporting Information is available free of charge at https://pubs.acs.org/doi/10.1021/acs.organomet.1c00244.

FTIR spectra of 6^{Ph}-C and 6^{Ph}-S, additional structural data and structure diagrams, summary of relevant crystallographic parameters, and NMR spectra (PDF)

Cartesian coordinates of the DFT optimized structures (XYZ)

Accession Codes

CCDC 2077801–2077807 contain the supplementary crystallographic data for this paper. These data can be obtained free of charge via www.ccdc.cam.ac.uk/data_request/cif, or by emailing data_request@ccdc.cam.ac.uk, or by contacting The Cambridge Crystallographic Data Centre, 12 Union Road, Cambridge CB2 1EZ, UK; fax: +44 1223 336033.

■ AUTHOR INFORMATION

Corresponding Authors

Jean-Cyrille Hierso − *Institut de Chimie Moléculaire de l'Université de Bourgogne (ICMUB) UMR CNRS 6302, Université Bourgogne Franche-Comté (UBFC), 21078 Dijon, France;* orcid.org/0000-0002-2048-647X; Email: jean-cyrille.hierso@u-bourgogne.fr

Petr Štěpnička − *Department of Inorganic Chemistry, Faculty of Science, Charles University, 128 40 Prague, Czech Republic;* orcid.org/0000-0002-5966-0578; Email: petr.stepnicka@natur.cuni.cz

Authors

Petr Vosáhlo − *Department of Inorganic Chemistry, Faculty of Science, Charles University, 128 40 Prague, Czech Republic*

Léa Radal − *Institut de Chimie Moléculaire de l'Université de Bourgogne (ICMUB) UMR CNRS 6302, Université Bourgogne Franche-Comté (UBFC), 21078 Dijon, France*

Marine Labonde − *Institut de Chimie Moléculaire de l'Université de Bourgogne (ICMUB) UMR CNRS 6302, Université Bourgogne Franche-Comté (UBFC), 21078 Dijon, France*

Ivana Císařová − *Department of Inorganic Chemistry, Faculty of Science, Charles University, 128 40 Prague, Czech Republic*

Julien Roger − *Institut de Chimie Moléculaire de l'Université de Bourgogne (ICMUB) UMR CNRS 6302, Université Bourgogne Franche-Comté (UBFC), 21078 Dijon, France;* orcid.org/0000-0002-4964-366X

Nadine Pirio − *Institut de Chimie Moléculaire de l'Université de Bourgogne (ICMUB) UMR CNRS 6302, Université Bourgogne Franche-Comté (UBFC), 21078 Dijon, France*

Complete contact information is available at: https://pubs.acs.org/10.1021/acs.organomet.1c00244

Notes

The authors declare no competing financial interest.

■ ACKNOWLEDGMENTS

This article is dedicated to Professor Pierre H. Dixneuf in recognition of his outstanding contributions to organometallic chemistry and catalysis. This work was supported by the Charles University Research Centre Programme (project UNCE/SCI/014). Computational resources were provided by the project "e-Infrastruktura CZ" (e-INFRA LM2018140) falling within the scheme Projects of Large Research, Development and Innovations Infrastructures. P.V. also thanks the Foundation of Faculty of Science, Charles University, for supporting his stay in Dijon. In Dijon, this work was supported by the ANR-PRC 2016 programme (ALCATRAS, ANR-16-CE07-0001-01), the CNRS, Université de Bourgogne, Conseil Régional de Bourgogne through the plan d'actions régional pour l'innovation (PARI), and the fonds européen de développement regional (FEDER). The authors also thank Dr. R. Gyepes from the Department of Inorganic Chemistry, Faculty of Science, Charles University, for valuable suggestions regarding DFT computations. Thanks are also due to Dr. H. Cattey from Institut de Chimie Moléculaire de l'Université de Bourgogne, Université Bourgogne Franche-Comté, for complementary crystallographic measurements.

■ REFERENCES

(1) *Catalysis: From Principles to Applications*, Beller, M., Renken, A., van Santen, R. A., Eds.; Wiley-VCH: 2012.

(2) *Phosphorus(III) Ligands in Homogeneous Catalysis: Design and Synthesis*; Kamer, P. C. J., van Leeuwen, P. W. N. M., Eds.; Wiley: 2012.

(3) (a) Bader, A.; Lindner, E. Coordination chemistry and catalysis with hemilabile oxygen-phosphorus ligands. *Coord. Chem. Rev.* **1991**, *108*, 27–110. (b) Slone, C. S.; Weinberger, D. A.; Mirkin, C. A. The Transition Metal Coordination Chemistry of Hemilabile Ligands. *Prog. Inorg. Chem.* **2007**, *48*, 233–350.

(4) (a) *Aqueous-Phase Organometallic Chemistry*, 2nd ed.; Cornils, B., Herrmann, W. A., Eds.; Wiley-VCH: 2004. (b) Pinault, N.; Bruce, D. W. Homogeneous catalysts based on water-soluble phosphines. *Coord. Chem. Rev.* **2003**, *241*, 1–25. (c) Shaughnessy, K. H. Hydrophilic Ligands and Their Application in Aqueous-Phase Metal-Catalyzed Reactions. *Chem. Rev.* **2009**, *109*, 643–710. (d) Butler, R. N.; Coyne, A. G. Water: Nature's Reaction Enforcer—Comparative Effects for Organic Synthesis "In-Water" and "On-Water. *Chem. Rev.* **2010**, *110*, 6302–6337. (e) Kitanosono, T.; Masuda, K.; Xu, P.; Kobayashi, S. Catalytic Organic Reactions in Water toward Sustainable Society. *Chem. Rev.* **2018**, *118*, 679–746.

(5) (a) Montalbetti, C. A. G. N.; Falque, V. Amide bond formation and peptide coupling. *Tetrahedron* **2005**, *61*, 10827–10852. (b) El-Faham, A.; Albericio, F. Peptide Coupling Reagents, More than a Letter Soup. *Chem. Rev.* **2011**, *111*, 6557–6602.

(6) Schulz, J.; Císařová, I.; Štěpnička, P. Phosphinoferrocene Amidosulfonates: Synthesis, Palladium Complexes, and Catalytic

Use in Pd-Catalyzed Cyanation of Aryl Bromides in an Aqueous Reaction Medium. *Organometallics* **2012**, *31*, 729−738.
(7) For alternative approaches toward the synthesis of phosphino-amidosulfonates, see: (a) Nuzzo, R. G.; Feitler, D.; Whitesides, G. M. Water-soluble complexes of tertiary phosphines and rhodium(I) as homogeneous catalysts. *J. Am. Chem. Soc.* **1979**, *101*, 3683−3685. (b) Nuzzo, R.; Haynie, S. L.; Wilson, M. E.; Whitesides, G. M. Synthesis of functional chelating diphosphines containing the bis[2-(diphenylphosphino)ethyl]amino moiety and the use of these materials in the preparation of water-soluble diphosphine complexes of transition metals. *J. Org. Chem.* **1981**, *46*, 2861−2867. (c) Fremy, G.; Castanet, Y.; Grzybek, R.; Monflier, E.; Morteux, A.; Trzeciak, A. M.; Ziolkowski, J. J. A new, highly selective, water-soluble rhodium catalyst for methyl acrylate hydroformylation. *J. Organomet. Chem.* **1995**, *505*, 11−16. (d) Lavenot, L.; Bortoletto, M. H.; Roucoux, A.; Larpent, C.; Patin, H. Synthesis of new hydrophilic phosphines by addition of diphenylphosphine on activated alkenes: characterization of their rhodium complexes. *J. Organomet. Chem.* **1996**, *509*, 9−14.
(8) (a) Štěpnička, P. Phosphino-carboxamides: the inconspicuous gems. *Chem. Soc. Rev.* **2012**, *41*, 4273−4305. (b) Štěpnička, P. Coordination and catalytic chemistry of phosphinoferrocene carboxamides. *Coord. Chem. Rev.* **2017**, *353*, 223−246.
(9) (a) Schulz, J.; Císařová, I.; Štěpnička, P. Synthesis of an amidosulfonate-tagged biphenyl phosphine and its application in the Suzuki-Miyaura reaction affording biphenyl-substituted amino acids in water. *J. Organomet. Chem.* **2015**, *796*, 65−72. (b) Schulz, J.; Horký, F.; Štěpnička, P. Different Performance of Two Isomeric Phosphinobiphenyl Amidosulfonates in Pd-Catalyzed Cyanation of Aryl Bromides. *Catalysts* **2016**, *6*, 182. (c) Schulz, J.; Horký, F.; Císařová, I.; Štěpnička, P. Synthesis, Structural Characterization and Catalytic Evaluation of Anionic Phosphinoferrocene Amidosulfonate Ligands. *Catalysts* **2017**, *7*, 167.
(10) (a) *Ferrocenes: Homogeneous Catalysis, Organic Synthesis, Materials Science*; Togni, A., Hayashi, T., Eds.; VCH: 1995. (b) *Ferrocenes: Ligands, Materials and Biomolecules*; Štěpnička, P., Ed.; Wiley: 2008. (c) Atkinson, R. C. J.; Gibson, V. C.; Long, N. J. The syntheses and catalytic applications of unsymmetrical ferrocene ligands. *Chem. Soc. Rev.* **2004**, *33*, 313−328. (d) Gómez Arrayás, R.; Adrio, J.; Carretero, J. C. Recent applications of chiral ferrocene ligands in asymmetric catalysis. *Angew. Chem., Int. Ed.* **2006**, *45*, 7674−7715.
(11) (a) Mom, S.; Beaupérin, M.; Roy, D.; Royer, S.; Amardeil, R.; Cattey, H.; Doucet, H.; Hierso, J.-C. Congested ferrocenyl polyphosphanes bearing electron-donating or electron-withdrawing phosphanyl groups: assessment of metallocene conformation from NMR spin couplings and use in palladium-catalyzed chloroarenes activation. *Inorg. Chem.* **2011**, *50*, 11592−11603. (b) Thomas, D. A.; Ivanov, V. V.; Butler, I. R.; Horton, P. N.; Meunier, P.; Hierso, J.-C. Coordination Chemistry of Tetra- and Tridentate Ferrocenyl Polyphosphines: An Unprecedented [1,1′-Heteroannular and 2,3-Homoannular]-Phosphorus-Bonding Framework in a Metallocene Dinuclear Coordination Complex. *Inorg. Chem.* **2008**, *47*, 1607−1615. (c) Beaupérin, M.; Smaliy, R.; Cattey, H.; Meunier, P.; Ou, J.; Toy, P. H.; Hierso, J.-C. Modular functionalized polyphosphines for supported materials: previously unobserved ^{31}P-NMR ABCD spin systems and heterogeneous palladium-catalysed C-C and C-H arylation. *Chem. Commun.* **2014**, *50*, 9505−9508.
(12) (a) Platon, M.; Roger, J.; Royer, S.; Hierso, J.-C. Palladium C-N bond formation catalyzed by air-stable robust polydentate ferrocenylphosphines: a comparative study for the efficient and selective coupling of aniline derivatives to dichloroarene. *Catal. Sci. Technol.* **2014**, *4*, 2072−2080. (b) Roger, J.; Mom, S.; Beaupérin, M.; Royer, S.; Meunier, P.; Ivanov, V. V.; Doucet, H.; Hierso, J.-C. Direct arylation of heterocycles: the performances of ferrocene-based polyphosphane ligands in palladium-catalyzed C-H bond activation. *ChemCatChem* **2010**, *2*, 296−305. (c) Platon, M.; Wijaya, N.; Rampazzi, V.; Cui, L.; Rousselin, Y.; Saeys, M.; Hierso, J.-C. Thioetherification of Chloroheteroarenes: A Binuclear Catalyst Promotes Wide Scope and High Functional-Group Tolerance. *Chem. - Eur. J.* **2014**, *20*, 12584−12594.
(13) (a) Evrard, D.; Lucas, D.; Mugnier, Y.; Meunier, P.; Hierso, J.-C. On the Mechanistic Behavior of Highly Efficient Palladium-Tetraphosphine Catalytic Systems for Cross-Coupling Reactions: First Spectroscopic and Electrochemical Studies of Oxidative Addition on Pd(0)/Multidentate Ferrocenylpolyphosphine Complexes. *Organometallics* **2008**, *27*, 2643−2653. (b) Zinovyeva, V. A.; Mom, S.; Fournier, S.; Devillers, C. H.; Cattey, H.; Doucet, H.; Hierso, J.-C.; Lucas, D. Kinetic and Electrochemical Studies of the Oxidative Addition of Demanding Organic Halides to Pd(0): the Efficiency of Polyphosphane Ligands in Low Palladium Loading Cross-Couplings Decrypted. *Inorg. Chem.* **2013**, *52*, 11923−11933.
(14) (a) Chanda, A.; Fokin, V. V. Organic Synthesis "On Water. *Chem. Rev.* **2009**, *109*, 725−748. (b) Kitanosono, T.; Kobayashi, S. Reactions in Water Involving the "On-Water" Mechanism. *Chem. - Eur. J.* **2020**, *26*, 9408−9429.
(15) Lerayer, E.; Renaut, P.; Roger, J.; Pirio, N.; Cattey, H.; Devillers, C.-H.; Lucas, D.; Hierso, J.-C. A general diastereoselective synthesis of highly functionalized ferrocenyl ambiphiles enabled on a large scale by electrochemical purification. *Chem. Commun.* **2017**, *53*, 6017−6020.
(16) Radal, L.; Vosáhlo, P.; Roger, J.; Cattey, H.; Amardeil, H.; Císařová, I.; Štěpnička, P.; Pirio, P.; Hierso, J.-C. Highly functionalized Brønsted acidic/Lewis basic hybrid ferrocene ligands: synthesis and coordination chemistry. *Eur. J. Inorg. Chem.* **2019**, *2019*, 865−874.
(17) Imamoto, T.; Oshiki, T.; Onozawa, T.; Kusumoto, T.; Sato, K. Synthesis and Reaction of phosphine-Boranes. Synthesis of New Bidentate Ligands with Homochiral Phosphine Centers via Optically Pure Phosphine-Boranes. *J. Am. Chem. Soc.* **1990**, *112*, 5244−5252. See also ref 9c.
(18) Tomasi, J.; Mennucci, B.; Cammi, R. Quantum Mechanical Continuum Solvation Models. *Chem. Rev.* **2005**, *105*, 2999−3093.
(19) (a) Aullón, G.; Alvarez, S. Axial Bonding Capabilities of Square Planar d^8-ML_4 Complexes. Theoretical Study and Structural Correlations. *Inorg. Chem.* **1996**, *35*, 3137−3144.
(20) (a) Platon, M.; Amardeil, R.; Djakovitch, L.; Hierso, J.-C. Progress in palladium-based catalytic systems for the sustainable synthesis of annulated heterocycles: a focus on indole backbones. *Chem. Soc. Rev.* **2012**, *41*, 3929−3968. (b) Humphrey, G. R.; Kuethe, J. T. Practical Methodologies for the Synthesis of Indoles. *Chem. Rev.* **2006**, *106*, 2875−2911. (c) Krüger, K.; Tillack, A.; Beller, M. Catalytic Synthesis of Indoles from Alkynes. *Adv. Synth. Catal.* **2008**, *350*, 2153−2167. (d) Vicente, R. Recent advances in indole syntheses: New routes for a classic target. *Org. Biomol. Chem.* **2011**, *9*, 6469−6480.
(21) Cacchi, S.; Fabrizi, G. Synthesis and Functionalization of Indoles Through Palladium-catalyzed Reactions. *Chem. Rev.* **2005**, *105*, 2873−2920.
(22) (a) Yamaguchi, A. D.; Itami, K. C−H Bond Functionalization: Emerging Synthetic Tools for Natural Products and Pharmaceuticals. *Angew. Chem., Int. Ed.* **2012**, *51*, 8960−9009. (b) Moncea, O.; Poinsot, D.; Fokin, A. A.; Schreiner, P. R.; Hierso, J.-C. Palladium-Catalyzed C2−H Arylation of Unprotected (N−H)-Indoles "On Water" Using Primary Diamantyl Phosphine Oxides as a Class of Primary Phosphine Oxide Ligands. *ChemCatChem* **2018**, *10*, 2915−2922. For examples exploiting substituted indoles and different arylating agents, see: (c) Zhu, Y.; Bauer, M.; Ackermann, L. Late-Stage Peptide Diversification by Bioorthogonal Catalytic C−H Arylation at 23 °C in H_2O. *Chem. - Eur. J.* **2015**, *21*, 9980−9983. (d) Reay, A. J.; Hammarback, L. A.; Bray, J. T. W.; Sheridan, T.; Turnbull, D.; Whitwood, A. C.; Fairlamb, I. J. S. Mild and Regioselective $Pd(OAc)_2$-Catalyzed C−H Arylation of Tryptophans by $[ArN_2]X$, Promoted by Tosic Acid. *ACS Catal.* **2017**, *7*, 5174−5179. (e) Vasudevan, N.; Wimmer, E.; Barré, E.; Cortés-Borda, D.; Rodriguez-Zubiri, M.; Felpin, F.-X. Direct C−H Arylation of Indole-3-Acetic Acid Derivatives Enabled by an Autonomous Self-Optimizing Flow Reactor. *Adv. Synth. Catal.* **2021**, *363*, 791−799.

https://doi.org/10.1021/acs.organomet.1c00244
Organometallics 2021, 40, 1934−1944

(23) Sheldrick, G. M. *SHELXT* – Integrated space-group and crystal-structure determination. *Acta Crystallogr., Sect. A: Found. Adv.* **2015**, *71*, 3−8.
(24) Sheldrick, G. M. Crystal structure refinement with *SHELXL*. *Acta Crystallogr., Sect. C: Struct. Chem.* **2015**, *71*, 3−8.
(25) Spek, A. L. *PLATON SQUEEZE*: a tool for the calculation of the disordered solvent contribution to the calculated structure factors. *Acta Crystallogr., Sect. C: Struct. Chem.* **2015**, *71*, 9−18.
(26) (a) Spek, A. L. Single-crystal structure validation with the program *PLATON*. *J. Appl. Crystallogr.* **2003**, *36*, 7−13. (b) Spek, A. L. Structure validation in chemical crystallography. *Acta Crystallogr., Sect. D: Biol. Crystallogr.* **2009**, *65*, 148−155.
(27) Frisch, M. J.; Trucks, G. W.; Schlegel, H. B.; Scuseria, G. E.; Robb, M. A.; Cheeseman, J. R.; Scalmani, G.; Barone, V.; Petersson, G. A.; Nakatsuji, H.; Li, X.; Caricato, M.; Marenich, A. V.; Bloino, J.; Janesko, B. G.; Gomperts, R.; Mennucci, B.; Hratchian, H. P.; Ortiz, J. V.; Izmaylov, A. F.; Sonnenberg, J. L.; Williams-Young, D.; Ding, F.; Lipparini, F.; Egidi, F.; Goings, J.; Peng, B.; Petrone, A.; Henderson, T.; Ranasinghe, D.; Zakrzewski, V. G.; Gao, J.; Rega, N.; Zheng, G.; Liang, W.; Hada, M.; Ehara, M.; Toyota, K.; Fukuda, R.; Hasegawa, J.; Ishida, M.; Nakajima, T.; Honda, Y.; Kitao, O.; Nakai, H.; Vreven, T.; Throssell, K.; Montgomery, J. A., Jr.; Peralta, J. E.; Ogliaro, F.; Bearpark, M. J.; Heyd, J. J.; Brothers, E. N.; Kudin, K. N.; Staroverov, V. N.; Keith, T. A.; Kobayashi, R.; Normand, J.; Raghavachari, K.; Rendell, A. P.; Burant, J. C.; Iyengar, S. S.; Tomasi, J.; Cossi, M.; Millam, J. M.; Klene, M.; Adamo, C.; Cammi, R.; Ochterski, J. W.; Martin, R. L.; Morokuma, K.; Farkas, O.; Foresman, J. B.; Fox, D. J. *Gaussian 16, Rev. C.01*, Gaussian, Inc.: 2016.
(28) Adamo, C.; Barone, V. Toward reliable density functional methods without adjustable parameters: The PBE0 model. *J. Chem. Phys.* **1999**, *110*, 6158−6170.
(29) (a) Dolg, M.; Wedig, U.; Stoll, H.; Preuss, H. Energy-adjusted *ab initio* pseudopotentials for the first row transition elements. *J. Chem. Phys.* **1987**, *86*, 866−872. (b) Andrae, D.; Häussermann, U.; Dolg, M.; Stoll, H.; Preuss, H. Energy-adjusted *ab initio* pseudopotentials for the second and third row transition elements. *Theor. Chim. Acta* **1990**, *77*, 123−141.
(30) Papajak, E.; Zheng, J.; Xu, X.; Leverentz, H. R.; Truhlar, D. G. Perspective on Basis Sets Beautiful: Seasonal Plantings of Diffuse Basis Functions. *J. Chem. Theory Comput.* **2011**, *7*, 3027−3034.

https://doi.org/10.1021/acs.organomet.1c00244
Organometallics 2021, 40, 1934−1944